Macromolecules

Article

# Wetting of Polymer Brushes by Polymeric Nanodroplets

Liz I. S. Mensink,[†] Jacco H. Snoeijer,[†] and Sissi de Beer*,[‡]

[†]Physics of Fluids, MESA+ Institute for Nanotechnology, and [‡]Materials Science and Technology of Polymers, MESA+ Institute for Nanotechnology, University of Twente, P.O. Box 217, 7500 AE Enschede, The Netherlands

S *Supporting Information*

ABSTRACT: End-anchoring polymers to a solid surface to form so-called polymer brushes is a versatile method to prepare robust functional coatings. We show, using molecular dynamics simulations, that these coatings display rich wetting behavior. Depending on the interaction between the brushes and the polymeric droplets as well as on the self-affinity of the brush, we can distinguish between three wetting states: mixing, complete wetting, and partial wetting. We find that transitions between these states are largely captured by enthalpic arguments, while deviations to these can be attributed to the negative excess interfacial entropy for the brush droplet system. Interestingly, we observe that the contact angle strongly increases when the softness of the brush is increased, which is opposite to the case of drops on soft elastomers. Hence, the Young to Neumann transition owing to softness is not universal but depends on the nature of the substrate.
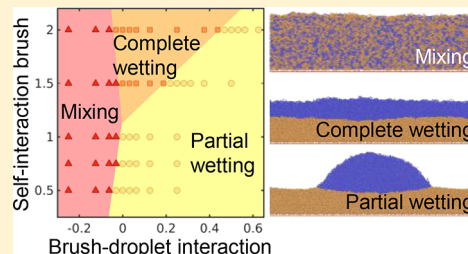
1. INTRODUCTION

Soft brushlike structures are found in multiple places in nature, for example in human joints, intestines, and lungs, where they aid in tasks such as lubrication, filtering, absorption, and antifouling.[1−3] In a biomimetic approach, most of these functionalities can be obtained by grafting polymers at a high density to a surface to form so-called polymer brushes.[4−7] Research interest in these polymer brushes has grown rapidly in recent years due to its potential for applications, e.g., as smart adhesives,[8−10] as sensors,[11−13] in gating,[14−16] in moisture management systems,[17,18] and on self-cleaning surfaces.[19,20] For many of these applications, it is important to understand how droplets interact with soft brush structures.

Recently, wetting of droplets on soft substrates has gained a lot of attention.[21−35] Wetting on these substrates can be very different from that on rigid substrates because surface tension can deform the substrates.[30,31,33] Considering the rigidity of the substrates, wetting behavior can be categorized in three regimes depending on the elastocapillary length, which is defined as the surface free energy γ divided by Young's modulus E. When γ/E is much smaller than the range of molecular interactions a, surfaces are not deformed and Young's law applies. When γ/E is larger than a, wetting ridges are formed,[21,23,34] which alter the microscopic contact angle yet do not affect the macroscopic contact angle θ. The macroscopic contact angle will deviate from predictions by Young's law only when γ/E is comparable to the droplet size R. For larger γ/E, θ becomes increasingly smaller and approaches Neumann's law in the limit of $\gamma/E \gg R$.[25−27]

For substrates composed of polymer brushes, one can anticipate even richer wetting behavior. The reason for this is that end-anchoring of the polymers imposes translational constraints that allow for wetting by liquids that would otherwise dissolve the polymers and thereby degrade the coating.[36] Moreover, the reduction of configurational entropy for surface-attached polymers can give rise to counterintuitive effects such as autophobic dewetting of chemically identical polymer films.[37−40] Previous work revealed the formation of wetting ridges for droplets on brushes.[41] However, so far, a complete overview of how brush softness in combination with brush−droplet affinity affects the wetting of brushes is still lacking.

In this article, we explore the wetting behavior of polymer brushes by polymer droplets under a wide variety of conditions. Using molecular dynamics simulations, we reveal three wetting states—mixing, complete wetting, and partial wetting—which can be controlled by the interactions between the brush polymers and the droplet relative to the interaction between the polymers in the brush. In the partial wetting state, we observe various phenomena that depend on the softness of the brush. Interestingly, we do not observe θ to decrease with increasing softness of the brush as observed for elastomers. Instead, we observe the opposite trend and that $\theta \to 180°$ for soft brushes.

2. MODEL AND METHODS

The polymers are represented by a coarse-grained bead−spring model (Kremer−Grest model[42]), which is known to capture the generic traits of bulk polymers,[43] polymers in solvent (mixtures),[44] and polymer brushes.[45,46] Within our Kremer−Grest based model, the nonbonded interactions within and between brush and liquid are described by a Lennard-Jones potential:

$$V_{LJ} = 4\epsilon \left(\left(\frac{\sigma}{r} \right)^{12} - \left(\frac{\sigma}{r} \right)^6 \right) \tag{1}$$

using $\sigma = 1$ and cut-off radius $r_c = 2.5\sigma$.[47] Within the Lennard-Jones potential, σ is the radius where the potential is zero and a representation for the size of the polymer bead. The parameter ϵ equals the potential well depth and is our unit of energy. The Lennard-Jones units can be translated to real values for polymers such as poly(ethylene) using $\epsilon = 30$ meV and $\sigma = 0.5$ nm.[43] Consecutive beads interact via the finite extensible nonlinear elastic (FENE) bond (spring stiffness $k = 30\epsilon/\sigma^2$ and maximum extent $R_0 = 1.5\sigma$), while overlap of the beads is inhibited by a Lennard-Jones potential that is cut off in the potential minimum (interaction strength $\epsilon = 1$, zero-crossing distance for the potential $\sigma = 1$, cutoff radius $r_c = 2^{1/6}\sigma$). A polymer bead represents typically 3−4 monomers. Therefore, the unit of mass $[m]$ is 10^{-22} kg and the unit of time $[\tau]$ represents 0.3 ns.[43]

The configurations shown in Figure 1a−c are extracted snapshots of our simulation cells.[48] The simulations are
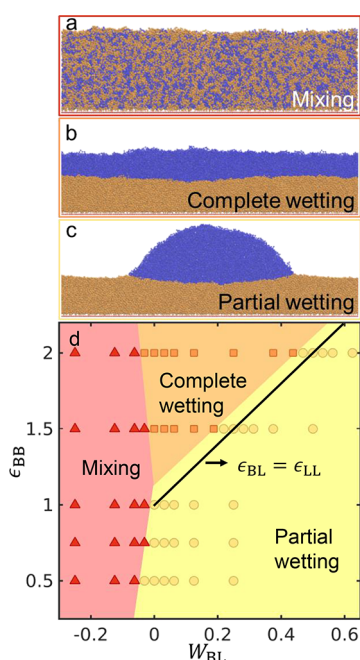

Figure 1. (a−c) Snapshots of simulation cells showing a polymer droplet (blue), interacting with a polymer brush (orange) for the three wetting states. (d) Phase diagram depicting the relation between the states of wetting and brush self-interaction ϵ_{BB} and the interaction parameter W_{BL}. Observed are mixing (red triangles), complete wetting (orange squares), and partial wetting states (yellow circles). The black line indicates the enthalpic prediction for the transition from complete to partial wetting ($\epsilon_{BL} = \epsilon_{LL}$).

performed at a constant box size (constant volume V) in a quasi-2D setup to prevent line-tension effects.[49] Boundary conditions are periodic in x and y, and the box length is limited to 15σ in y to suppress the Rayleigh instability in the infinitely long cylindrical droplet (Figure 1c). All simulation cells contain surfaces with high density polymer brushes attached to them (orange, Figure 1). The grafting density is 0.15 chains per unit area, which is 20× the critical grafting density for brush formation.[50] This density is in the high density regime[51] as is commonly obtained in laboratories using the "grafting

from" method.[8,52] Each brush polymer consists of $N_B = 100$ repeat units and is allowed to interact with a droplet containing 485 polymers, each of $N_L = 32$ repeat units (blue, Figure 1).

The equations of motion are solved using the Verlet algorithm as implemented in LAMMPS[53] using a time step of $\Delta t = 0.005\tau$. The simulations are performed in the NVT ensemble, and the temperature T is kept constant at $k_B T = 1\epsilon$ (k_B being the Boltzmann constant) using a Langevin thermostat (damping coefficient $\xi = 1\tau^{-1}$). We vary ϵ_{BB} between 0.5 and 2. By varying ϵ_{BB}, we vary implicitly the interaction of the brush with the implicit solvent. When ϵ_{BB} is high, the brush polymers like themselves and, thereby, dislike the implicit solvent. In contrast, when ϵ_{BB} is low, the self-interaction within the brush polymers is low, and the polymers prefer the implicit solvent. The variation in ϵ_{BB} can be related to effective self-interaction parameters $\tau_s = \epsilon_{BB}/\epsilon_{BB,\theta}$ between 1.6 and 6.5. In this equation $\epsilon_{BB,\theta} = 0.31$ is the θ-transition point, below which the brush is in implicit good solvent conditions. We employ a generic LJ interaction and do not intend to model particular types of polymers. Moreover, we do not limit ourselves to systems described by van der Waals interactions alone. Therefore, mixing rules are not strict,[54] and we can alter ϵ_{BB} and ϵ_{BL} independently. This will make our results broadly applicable. We vary ϵ_{BL} between 0.125 and 1.75, while $\epsilon_{LL} = 1$ is kept constant. In experiments these interactions can be altered by choosing different combinations of polymers. The interactions between the wall and the polymer or liquid beads is purely repulsive ($\epsilon = 1$, $\sigma = 1$, and $r_c = 2^{1/6}\sigma$) to prevent preferential adsorption near the wall.[55] Because of our choice for the wall interactions as well as the thickness of our polymer film, there will also be no wall-induced wetting transitions.[56]

3. RESULTS AND DISCUSSION

The phase diagram of Figure 1d depicts how the wetting regimes depend on the affinity of the brush with the droplet (x-axis) as well as the self-interaction of the brush ϵ_{BB} (y-axis). The brush−droplet affinity is characterized by the interaction parameter W_{BL}, which we define as $W_{BL} = \frac{1}{2}(\epsilon_{BB} + \epsilon_{LL}) - \epsilon_{BL}$. It gives the droplet−brush affinity relative to the self-interactions within the droplet and the brush. Our W_{BL} can be related to the traditional Flory−Huggins parameter;[57] for more information about this translation we refer to refs 58 and 59. The swelling of the brushes is controlled by ϵ_{BB}. A large ϵ_{BB} models a hard, rigid brush, while a small ϵ_{BB} results in a softer brush.

We first focus on the red region of the phase diagram in Figure 1d, where the interactions are such that deposited droplets mix with the brush polymers. Depending on ϵ_{BB}, different melt partitioning regimes can be identified. We observe that the composition of the brush air interface varies between melt-enriched for large ϵ_{BB} (see Figure 2a for $\epsilon_{BB} = 2\epsilon_{LL}$) to brush-enriched for small ϵ_{BB} (see Figure 2b for $\epsilon_{BB} = 0.5\epsilon_{LL}$). The latter regime has also been predicted by self-consistent field theory calculations.[60] The reason for such a nonuniform distribution and variation in interfacial composition is that the medium with the lower self-affinity will pay a smaller energy penalty for residing at the interface.

Upon increasing W_{BL}, we observe a transition from mixing to partial wetting for small ϵ_{BB} and to complete wetting for large ϵ_{BB}. To identify the exact transition W_{BL} ($W_{BL,TR}$), we calculate the binary interaction count N_{int} (see the Supporting Information),[61] which is high for mixing systems and low for phase-separated systems. We define N_{int} as
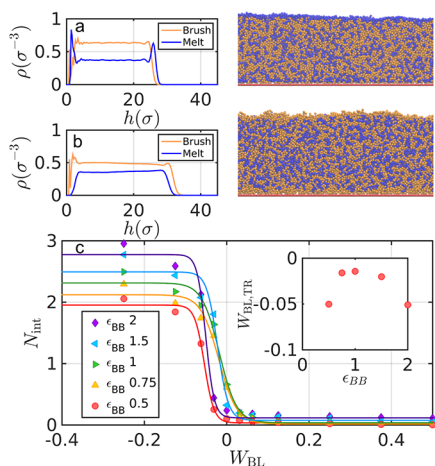
Figure 2. (a, b) Density profiles of a polymer melt (blue) mixed into a polymer brush (orange); (a) shows mixing in a collapsed brush ($\epsilon_{BB} = 2\epsilon_{LL}$), and (b) shows mixing in an initially slightly extended brush ($\epsilon_{BB} = 0.5\epsilon_{LL}$). (c) Binary interaction count for different polymer brushes (ϵ_{BB}, given in the legend) interacting with a polymer liquid for different interaction parameters W_{BL}. The inset shows the transition W_{BL}.

$$N_{int} = \frac{1}{N_{BU}} \sum_{i=1}^{N_{BU}} \sum_{j=1}^{N_{LU}} H(r_{ij} - r_c)$$

where N_{BU} is the total number of brush units in the simulation cell, N_{LU} is the total number of liquid units, and $H(r_{ij} - r_c)$ is a Heaviside function, which is 1 when the interparticle distance r_{ij} is smaller than $r_c = 1.5\sigma$.

Figure 2c shows N_{int} for various ϵ_{BB} between 0.5 and 2. We define $W_{BL,TR}$ as the halfway point of the hyperbolic tangent fitted to the data. The $W_{BL,TR}$ is negative for all ϵ_{BB} (see the inset in Figure 2c). A negative $W_{BL,TR}$ might seem counterintuitive because this implies that mixing reduces the entropy of the system. However, it can be understood using similar arguments as for autophobic dewetting.[37] The reason for the observed effect is that end-anchored polymers are constrained, and therefore they do not gain translational entropy upon mixing. Instead, they pay an entropic penalty for stretching when absorbing the polymer melt. If the polymers in the melt are sufficiently long, their gain in translational entropy upon absorption in the brush is too small to overcome the reduction in entropy due to stretching of the polymers of the brush such that the system will not mix. This is consistent with previous studies on mixing/demixing of brushes with chemically identical melts,[62,63] which suggest a demixed state at $W_{BL} = 0$ for our grafting density and $N_L/N_B = 0.35$. Therefore, our mixing–demixing transitions have to occur at negative W_{BL}.

In contrast to predictions,[64] the observed $W_{BL,TR}$ is not constant. Instead, it increases with increasing ϵ_{BB} for $\epsilon_{BB} < 0.75\epsilon_{LL}$, while it decreases with increasing ϵ_{BB} for $\epsilon_{BB} > 1\epsilon_{LL}$ (see the inset in Figure 2c). This demonstrates that Flory–Huggins or scaling theories cannot be directly applied to our system. The reason for this is that the volume conservation and the incompressibility assumptions are invalid due to the compressibility of the implicit solvent. Indeed, inspection of the average densities of the liquid and the brush reveals that mixing alters the average free volume. Similar conditions apply in the lab, where the droplet and brush are in equilibrium with (compressible) air.

Now we turn to the right side of the phase diagram of Figure 1d, where the melt and the brush do not mix. In the orange region of the phase diagram, the liquid completely wets the brush, while in the yellow region, the melt partially wets the brush and takes the shape of a droplet. It is possible to link the transition between partial and complete wetting for our brush system to the well-known wetting transition for nonabsorbing surfaces described by the Young–Dupré law. For this, we relate the spreading parameter S defined by the solid–liquid, solid–vapor, and liquid–vapor surface tensions—γ_{SL}, γ_{SV}, and γ_{LV}, respectively—to the interaction parameter ϵ. This relation can be found considering the work of adhesion upon separation, which is proportional to the strength of the interaction ϵ between the media before separation.[54] Upon separating two half-space media, two new interfaces between the media and the air (vapor) are created, each of which has a surface energy γ. If the two media consist of the same liquid, the work of adhesion $W = 2\gamma_{LV}$, and this must be proportional to ϵ_{LL}. Similarly, for the same (brush) solids $W = 2\gamma_{SV}$, and this expression scales with ϵ_{BB}. If a (brush) solid and a liquid are separated, we need to correct for the initial interfacial energy γ_{SL} such that $W = \gamma_{SV} + \gamma_{LV} - \gamma_{SL}$, and this should scale with ϵ_{BL}. By these enthalpic considerations, the spreading parameter becomes $S = \gamma_{SV} - (\gamma_{SL} + \gamma_{LV}) \propto \epsilon_{BL} - \epsilon_{LL}$. When $S < 0$ the liquid partially wets the surface, while for $S > 0$ complete wetting occurs. Therefore, the partial to complete wetting transition is expected to occur at $\epsilon_{BL} = \epsilon_{LL}$ if enthalpic interactions determine the transition. Moreover, using Young's law for $S < 0$, we can write $S = \gamma_{LV}(\cos \theta - 1)$, which leads to the estimation for the contact angle as $\cos \theta = 2\epsilon_{BL}/\epsilon_{LL} - 1$.

Comparing the model predicting the partial to complete wetting transition ($\epsilon_{BL} = \epsilon_{LL}$, black line Figure 1d) with the simulation results (orange and yellow in Figure 1d; see the Supporting Information for typical snapshots near the transition), we find a reasonable qualitative agreement. However, it is clear that this transition is shifted to smaller W_{BL} for all ϵ_{BB}. The reason for this shift has the same roots as the shift in $W_{BL,TR}$: it can be attributed to the entropic penalty that our setup pays for mixing.[37,62] The entropic penalty, or negative excess entropy, increases the effective interfacial free energy between the brush and the liquid, γ_{SL}.[65,66] This increase in γ_{SL} reduces the spreading parameter S such that partial wetting is observed for $\epsilon_{BL} = \epsilon_{LL}$. The latter has been confirmed with experiments of autophobic dewetting, where indeed finite contact angles are observed for melt droplets on the chemically identical high-density brushes.[39,67,68] This shows that our setup models experimental systems reasonably well, despite our system size being smaller. Moreover, preliminary tests show that the transition shift and, thus, the entropic contribution to the interfacial free energy strongly depend on the degree of polymerization of the droplet polymers N_L, in agreement with experimental observations.[39]

To further examine the partial wetting state, we determine the contact angles of the droplets on the brushes (see Figure 3). The contact angle is extracted by spherical fits to the top part of the droplet that rises above the height of the unperturbed brush. Figure 3 shows the contact angles θ for brush–droplet combinations in the partial wetting regime. We plot θ extracted from the simulations as a function of the contact angle predicted from the enthalpic model for Young's law, $\cos \theta = 2\epsilon_{BL}/\epsilon_{LL} - 1$. The contact angles extracted from the simulations are always more than 20° higher than expected from enthalpic interactions. This increase in the contact angle
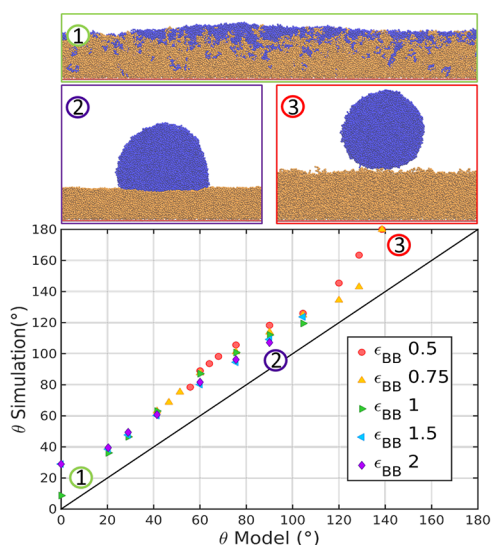
Figure 3. Snapshots 1−3 show the typical partial wetting states with the corresponding numbering referring to their data points in the graph. Below is a plot of the contact angles extracted from the simulations versus the contact angles predicted from enthalpic arguments. The individual series are at constant ϵ_{BB} (given in the legend) and are all varied in ϵ_{BL}.

can also largely be explained by the entropic penalty-induced increase in γ_{SL},[65,66] which will effectively increase the contact angle.

For the snapshots in Figure 3, we can distinguish between three partial wetting regimes depending on ϵ_{BB} and ϵ_{BL}. For $\epsilon_{BB} > 1$, the brush surface is not deformed by the surface tension of the droplet (see Figure 3, snapshot 2). In this regime, Young's law should be valid when entropic contributions are taken into account. For $\epsilon_{BB} \leq 1$, the brush is soft enough such that wetting ridges are formed (see Figure S2), consistent with observations by Léonforte et al.[41] The height of the wetting ridges slightly increases from 4σ to 5σ upon decreasing ϵ_{BB} from 1 to 0.5 (see the Supporting Information) because a reduction in ϵ_{BB} decreases the stiffness of the brush. The height of the ridges also increases (∼300%) with increasing ϵ_{BL} from 0.5 to 0.75 because this reduces γ_{SL}, counteracting the deformation.

In contrast to reports on droplets on soft gels,[25,26] we observe no Young to Neumann transition and the according decrease in contact angles for soft brushes and high γ_{SL}. Instead, we observe an increase in the contact angle to even 180° for small ϵ_{BB} and ϵ_{BL} (see Figure 3, snapshot 3). This is surprising because the effect cannot be attributed to the deformability of the substrate and should, therefore, be caused by the interactions. However, ϵ_{BB} does not affect Young's law estimated from enthalpic arguments. To understand our observed trend in θ, we have to consider that we have three components in our system and that the brush−melt interactions are mediated by the implicit solvent. By reducing ϵ_{BB}, we increase the affinity of the brush with the implicit solvent, such that we effectively reduce the affinity of the brush with the polymer droplet. This increases the contact angle. Moreover, at low ϵ_{BB}, the density of the brush decays with the distance from the surface, such that the droplet's inclusion free energy, which strongly increases with the density of the brush,[46] is the lowest in the top of the brush. Therefore, the melt is expelled to the top of the brush. Our results imply that

the Young to Neumann transition is not universal. However, the results do not exclude that such a transition could still occur for softer brushes of lower grafting densities.

4. CONCLUSIONS

In summary, we have shown that there are three wetting states for polymeric nanodroplets in contact with brushes: mixing, complete wetting, and partial wetting. The transitions between mixing and demixing and partial and complete wetting are largely determined by enthalpic interactions. However, detailed examination reveals significant entropy-induced deviations. The transition W_{BL} for mixing is always slightly negative, independent of the self-affinity of the brush ϵ_{BB}. This implies that there is a decrease in entropy upon mixing for our choice of system parameters (polymer length and grafting density). This effect is caused by the entropic penalty for stretching of the brush polymers upon mixing, which is not sufficiently compensated for by the gain in translational entropy of the melt polymers. Above the transition W_{BL}, we observe complete wetting for large ϵ_{BB} and partial wetting for small ϵ_{BB}. Also, the transition from partial to complete wetting is shifted to smaller W_{BL} than expected from the Young−Dupré equation considering only enthalpic interactions. The reason for this is that the negative excess interfacial entropy between the brush and the droplet effectively increases the interfacial free energy γ_{SL} between them. As a consequence, the contact angles extracted from the simulations in the partial wetting regime are also consistently higher than expected from Young's law considering only enthalpic interactions. Interestingly, we find that in the limit of high γ_{SL} and low brush stiffness contact angles increase and approach 180°. This is the opposite of what is generally reported for droplets in contact with soft gels, where contact angles are observed to decrease under these conditions. This reveals that the Young to Neumann transition owing to softness cannot be considered as universal: It depends on the specific nature of the substrate. These observations will impact the design and functionality of soft surfaces in terms of wetting and adhesive performance.

■ ASSOCIATED CONTENT

ⓢ Supporting Information

The Supporting Information is available free of charge on the ACS Publications website at DOI: 10.1021/acs.macromol.8b02409.

> Snapshots near the transition point and snapshots of the wetting ridges (PDF)

■ AUTHOR INFORMATION

Corresponding Author

*E-mail s.j.a.debeer@utwente.nl; phone +31 (0) 53 489 3170.

ORCID ⓘ

Sissi de Beer: 0000-0002-7208-6814

Notes

The authors declare no competing financial interest.

■ ACKNOWLEDGMENTS

■ REFERENCES

(1) Klein, J. Repair or Replacement—A Joint Perspective. *Science* **2009**, *323*, 47.

(2) Johansson, M. E. V.; Ambort, D.; Pelaseyed, T.; Schütte, A.; Gustafsson, J. K.; Ermund, A.; Subramani, D. B.; Holmén-Larsson, J. M.; Thomsson, K. A.; Bergström, J. H.; Van Der Post, S.; Rodriguez-Piñeiro, A. M.; Sjövall, H.; Bäckström, M.; Hansson, G. C. Composition and functional role of the mucus layers in the intestine. *Cell. Mol. Life Sci.* **2011**, *68*, 3635−3641.

(3) Button, B.; Cai, L.-H.; Ehre, C.; Kesimer, M.; Hill, D. B.; Sheehan, J. K.; Boucher, R. C.; Rubinstein, M. A Periciliary Brush Promotes the Lung Health by Separating the Mucus Layer from Airway Epithelia. *Science* **2012**, *337*, 937−941.

(4) Balazs, A. C.; Emrick, T.; Russell, T. P. Nanoparticle polymer composites: where two small worlds meet. *Science* **2006**, *314*, 1107−1110.

(5) Chen, M.; Briscoe, W. H.; Armes, S. P.; Klein, J. Lubrication at physiological pressures by polyzwitterionic brushes. *Science* **2009**, *323*, 1698−1701.

(6) Hucknall, A.; Rangarajan, S.; Chilkoti, A. In Pursuit of Zero: Polymer Brushes that Resist the Adsorption of Proteins. *Adv. Mater.* **2009**, *21*, 2441−2446.

(7) de Beer, S.; Kutnyanszky, E.; Schön, P. M.; Vancso, G. J.; Müser, M. H. Solvent-induced immiscibility of polymer brushes eliminates dissipation channels. *Nat. Commun.* **2014**, *5*, 3781.

(8) Yu, Y.; Kieviet, B. D.; Kutnyanszky, E.; Vancso, G. J.; de Beer, S. Cosolvency-Induced Switching of the Adhesion between Poly(methyl methacrylate) Brushes. *ACS Macro Lett.* **2015**, *4*, 75.

(9) Yu, Y.; Lopez de la Cruz, R. A.; Kieviet, B. D.; Gojzewski, H.; Pons, A.; Vancso, G. J.; de Beer, S. Pick up move and release of nanoparticles utilizing co-non-solvency of PNIPAM brushes. *Nanoscale* **2017**, *9*, 1670−1675.

(10) Cao, Z.; Bian, Q.; Chen, Y.; Liang, F.; Wang, G. Light-Responsive Janus-Particle-Based Coatings for Cell Capture and Release. *ACS Macro Lett.* **2017**, *6*, 1124−1128.

(11) Tokareva, I.; Minko, S.; Fendler, J. H.; Hutter, E. Nanosensors based on responsive polymer brushes and gold nanoparticle enhanced transmission surface plasmon resonance spectroscopy. *J. Am. Chem. Soc.* **2004**, *126*, 15950.

(12) Merlitz, H.; He, G.-L.; Wu, C.-X.; Sommer, J.-U. Nanoscale brushes: How to build a smart surface coating. *Phys. Rev. Lett.* **2009**, *102*, 115702.

(13) Klushin, L. I.; Skvortsov, A. M.; Polotsky, A. A.; Qi, S.; Schmid, F. Sharp and Fast: Sensors and Switches Based on Polymer Brushes with Adsorption-Active Minority Chains. *Phys. Rev. Lett.* **2014**, *113*, 068303.

(14) Jovanovic-Talisman, T.; Tetenbaum-Novatt, J.; McKenney, A. S.; Zilman, A.; Peters, R.; Rout, M. P.; Chait, B. T. Artificial nanopores that mimic the transport selectivity of the nuclear pore complex. *Nature* **2009**, *457*, 1023.

(15) Tagliazucchi, M.; Peleg, O.; Kröger, M.; Rabin, Y.; Szleifer, I. Effect of charge, hydrophobicity, and sequence of nucleoporins on the translocation of model particles through the nuclear pore complex. *Proc. Natl. Acad. Sci. U. S. A.* **2013**, *110*, 3363.

(16) Zhang, Y.; Mulvenna, R. A.; Qu, S.; Boudouris, B. W.; Phillip, W. A. Block Polymer Membranes Functionalized with Nanoconfined Polyelectrolyte Brushes Achieve Sub-Nanometer Selectivity. *ACS Macro Lett.* **2017**, *6*, 726−732.

(17) Yang, H.; Zhu, H.; Hendrix, M. M. R. M.; Lousberg, N. J. H. G. M.; de With, G.; Esteves, A. C. C.; Xin, J. H. Temperature-Triggered Collection and Release of Water from Fogs by a Sponge-Like Cotton Fabric. *Adv. Mater.* **2013**, *25*, 1150−1154.

(18) Liu, X.; Li, Y.; Hu, J.; Jiao, J.; Li, J. Smart moisture management and thermoregulation properties of stimuli-responsive cotton modified with polymer brushes. *RSC Adv.* **2014**, *4*, 63691−63695.

(19) Azzaroni, O.; Brown, A. A.; Huck, W. T. S. UCST wetting transitions of polyzwitterionic brushes driven by self-association. *Angew. Chem., Int. Ed.* **2006**, *45*, 1770.

(20) Howarter, J. A.; Youngblood, J. P. Self-Cleaning and Anti-Fog Surfaces via Stimuli-Responsive Polymer Brushes. *Adv. Mater.* **2007**, *19*, 3838−3843.

(21) Shanahan, M. E. R. The influence of solid micro-deformation on contact angle equilibrium. *J. Phys. D: Appl. Phys.* **1987**, *20*, 945.

(22) Carré, A.; Gastel, J.-C.; Shanahan, M. E. R. Visco-elastic effects in spreading of liquids. *Nature* **1996**, *379*, 432−434.

(23) Jerison, E. R.; Xu, Y.; Wilen, L. A.; Dufresne, E. R. Deformation of an Elastic Substrate by a Three-Phase Contact Line. *Phys. Rev. Lett.* **2011**, *106*, 186103.

(24) Kajiya, T.; Daerr, A.; Narita, T.; Royon, L.; Lequeux, F.; Limat, L. Advancing liquid contact line on visco-elastic gel substrates: stick-slip vs. continuous motions. *Soft Matter* **2013**, *9*, 454−461.

(25) Lubbers, L.; Weijs, J.; Botto, L.; Das, S.; Andreotti, B.; Snoeijer, J. Drops on soft solids: free energy and double transition of contact angles. *J. Fluid Mech.* **2014**, *747*, R1−12.

(26) Cao, Z.; Dobrynin, A. V. Polymeric Droplets on Soft Surfaces: From Neumann's Triangle to Young's Law. *Macromolecules* **2015**, *48*, 443−451.

(27) Dervaux, J.; Limat, L. Contact lines on soft solids with uniform surface tension: analytical solutions and double transition for increasing deformability. *Proc. R. Soc. London, Ser. A* **2015**, *471*, 20140813.

(28) Karpitschka, S.; Das, S.; van Gorcum, M.; Perrin, H.; Andreotti, B.; Snoeijer, J. H. Droplets move over viscoelastic substrates by surfing a ridge. *Nat. Commun.* **2015**, *6*, 7891.

(29) Karpitschka, S.; Pandey, A.; Lubbers, L. A.; Weijs, J. H.; Botto, L.; Das, S.; Andreotti, B.; Snoeijer, J. H. Liquid drops attract or repel by the inverted Cheerios effect. *Proc. Natl. Acad. Sci. U. S. A.* **2016**, *113*, 7403−7407.

(30) Andreotti, B.; Baumchen, O.; Boulogne, F.; Daniels, K. E.; Dufresne, E. R.; Perrin, H.; Salez, T.; Snoeijer, J. H.; Style, R. W. Solid capillarity: when and how does surface tension deform soft solids? *Soft Matter* **2016**, *12*, 2993−2996.

(31) Style, R. W.; Jagota, A.; Hui, C.-Y.; Dufresne, E. R. Elastocapillarity: Surface Tension and the Mechanics of Soft Solids. *Annu. Rev. Condens. Matter Phys.* **2017**, *8*, 99−118.

(32) Xu, Q.; Jensen, K.; Boltyanskiy, R.; Sarfati, R.; Style, R. W.; Dufresne, E. R. Direct measurement of strain-dependent solid surface stress. *Nat. Commun.* **2017**, *8*, 555.

(33) Bico, J.; Reyssat, E.; Roman, B. Elastocapillarity: When Surface Tension Deforms Elastic Solids. *Annu. Rev. Fluid Mech.* **2018**, *50*, 629−659.

(34) Liang, H.; Cao, Z.; Wang, Z.; Dobrynin, A. V. Surface Stresses and a Force Balance at a Contact Line. *Langmuir* **2018**, *34*, 7497−7502.

(35) Schulman, R. D.; Trejo, M.; Salez, T.; Raphael, E.; Dalnoki-Veress, K. Surface energy of strained amorphous solids. *Nat. Commun.* **2018**, *9*, 982.

(36) Lequeux, F.; Talini, L.; Verneuil, E.; Delannoy, G.; Valois, P. Wetting of polymers by their solvents. *Eur. Phys. J. E: Soft Matter Biol. Phys.* **2016**, *39*, 12.

(37) de Gennes, P. G. Conformations of polymers attached to an interface. *Macromolecules* **1980**, *13*, 1069.

(38) Ferreira, P. G.; Ajdari, A.; Leibler, L. Scaling Law for Entropic Effects at Interfaces between Grafted Layers and Polymer Melts. *Macromolecules* **1998**, *31*, 3994−4003.

(39) Maas, J. H.; Fleer, G. J.; Leermakers, F. A. M.; Cohen Stuart, M. A. Wetting of a polymer brush by a chemically identical polymer melt: Phase diagram and film stability. *Langmuir* **2002**, *18*, 8871−8880.

(40) Pastorino, C.; Binder, K.; Kreer, T.; Müller, M. Static and dynamic properties of the interface between a polymer brush and a melt of identical chains. *J. Chem. Phys.* **2006**, *124*, 064902.

(41) Léonforte, F.; Müller, M. Statics of polymer droplets on deformable surfaces. *J. Chem. Phys.* **2011**, *135*, 214703.

(42) Grest, G. S.; Kremer, K. Molecular dynamics simulation for polymers in the presence of a heat bath. *Phys. Rev. A: At., Mol., Opt. Phys.* **1986**, *33*, 3628.

(43) Kremer, K.; Grest, G. S. Dynamics of entangled linear polymer melts: A molecular-dynamics simulation. *J. Chem. Phys.* **1990**, *92*, 5057.

(44) Mukherji, D.; Marques, C. M.; Kremer, K. Collapse in two good solvents, swelling in two poor solvents: defying the laws of polymer solubility? *J. Phys.: Condens. Matter* **2018**, *30*, 024002.

(45) de Beer, S.; Müser, M. H. Friction in (Im-) Miscible Polymer Brush Systems and the Role of Transverse Polymer Tilting. *Macromolecules* **2014**, *47*, 7666.

(46) de Beer, S.; Mensink, L. I. S.; Kieviet, B. D. Geometry-Dependent Insertion Forces on Particles in Swollen Polymer Brushes. *Macromolecules* **2016**, *49*, 1070−1078.

(47) Throughout the paper we will employ Lennard-Jones units, with σ being the unit of length, ϵ being the unit of energy, and τ being the unit of time.

(48) Humphrey, W.; Dalke, A.; Schulten, K. VMD - Visual Molecular Dynamics. *J. Mol. Graphics* **1996**, *14*, 33.

(49) Weijs, J. H.; Marchand, A.; Andreotti, B.; Lohse, D.; Snoeijer, J. H. Origin of line tension for a Lennard-Jones nanodroplet. *Phys. Fluids* **2011**, *23*, 022001.

(50) Brittain, W. J.; Minko, S. A Structural Definition of Polymer Brushes. *J. Polym. Sci., Part A: Polym. Chem.* **2007**, *45*, 3505.

(51) Coluzza, I.; Hansen, J.-P. Transition from Highly to Fully Stretched Polymer Brushes in Good Solvent. *Phys. Rev. Lett.* **2008**, *100*, 016104.

(52) Zdyrko, B.; Klep, V.; Luzinov, I. Synthesis and Surface Morphology of High-Density Poly(ethylene glycol) Grafted Layers. *Langmuir* **2003**, *19*, 10179−10187.

(53) Plimpton, S. Fast Parallel Algorithms for Short-Range Molecular Dynamics. *J. Comput. Phys.* **1995**, *117*, 1.

(54) Israelachvili, J. N. *Intermolecular and Surface Forces*; Academic Press: New York, 2011.

(55) Descas, R.; Sommer, J.-U.; Blumen, A. Grafted polymer chains interacting with substrates: computer simulations and scaling. *Macromol. Theory Simul.* **2008**, *17*, 429.

(56) MacDowell, L. G.; Müller, M. Adsorption of polymers on a brush: Tuning the order of the wetting phase transition. *J. Chem. Phys.* **2006**, *124*, 084907.

(57) Flory, P. J. *Principles of Polymer Chemistry*; Cornell University Press: Ithaca, NY, 1953.

(58) Heine, D. R.; Grest, G. S.; Curro, J. G. Structure of Polymer Melts and Blends: Comparison of Integral Equation Theory and Computer Simulations. *Adv. Polym. Sci.* **2005**, *173*, 209.

(59) Zhang, W.; Gomez, E. D.; Milner, S. T. Predicting Flory-Huggins χ from Simulations. *Phys. Rev. Lett.* **2017**, *119*, 017801.

(60) Cohen Stuart, M. A.; de Vos, W. M.; Leermakers, F. A. M. Why Surfaces Modified by Flexible Polymers Often Have a Finite Contact Angle for Good Solvents. *Langmuir* **2006**, *22*, 1722−1728.

(61) Kreer, T.; Binder, K.; Müser, M. H. Friction between polymer brushes in good solvent conditions: steady-state sliding versus transient behavior. *Langmuir* **2003**, *19*, 7551.

(62) Aubouy, M.; Fredrickson, G. H.; Pincus, P.; Raphaël, E. End-Tethered Chains in Polymeric Matrixes. *Macromolecules* **1995**, *28*, 2979−2981.

(63) Grest, G. S. Grafted polymer brushes in polymeric matrices. *J. Chem. Phys.* **1996**, *105*, 5532−5541.

(64) Aubouy, M.; Raphael, E. Surface-Tethered Chains in Polymeric Matrixes. *J. Phys. II* **1993**, *3*, 443−448.

(65) Reiter, G.; Khanna, R. Negative Excess Interfacial Entropy between Free and End-Grafted Chemically Identical Polymers. *Phys. Rev. Lett.* **2000**, *85*, 5599−5602.

(66) Matsen, M. W.; Gardiner, J. M. Autophobic dewetting of homopolymer on a brush and entropic attraction between opposing brushes in a homopolymer matrix. *J. Chem. Phys.* **2001**, *115*, 2794−2804.

(67) Zhang, X.; Lee, F. K.; Tsui, O. K. C. Wettability of End-Grafted Polymer Brush by Chemically Identical Polymer Films. *Macromolecules* **2008**, *41*, 8148−8151.

(68) Lee, H.; Sethuraman, V.; Kim, Y.; Lee, W.; Ryu, D. Y.; Ganesan, V. Nonmonotonic Glass Transition Temperature of Polymer Films Supported on Polymer Brushes. *Macromolecules* **2018**, *51*, 4451−4461.